# Smectic Ordering of Parallel Hard Spherocylinders: An Entropy-Based Monte Carlo Study

**D. Costa,[†] F. Saija,[‡] and P. V. Giaquinta*[,†]**

*Dipartimento di Fisica, Istituto Nazionale per la Fisica della Materia (INFM) and Università degli Studi di Messina, Contrada Papardo, C.P. 50-98166 Messina, Italy, and Istituto per i Processi Chimico-Fisici, CNR, sez. Messina, Via La Farina, 237-98123 Messina, Italy*

*Received: February 27, 2003; In Final Form: May 26, 2003*

We investigated the nematic to smectic transition undergone by parallel hard spherocylinders in the framework provided by the residual multiparticle entropy (RMPE) formalism. The RMPE is defined as the sum of all contributions to the configurational entropy of the fluid that arise from density correlations involving more than two particles. The vanishing of the RMPE signals the structural changes that take place in the system for increasing pressures. Monte Carlo simulations carried out for parallel hard spherocylinders show that such a one-phase ordering criterion accurately predicts also the nematic−smectic transition threshold notwithstanding the almost continuous character of the transition. A similar quantitative correspondence had been already noted in the case of an isotropic fluid of freely rotating hard spherocylinders undergoing a transition to a nematic, smectic, or solid phase. The present analysis confirms the flexibility of the RMPE approach as a practical and reliable tool for detecting the formation of mesophases in model liquid crystals.

## 1. Introduction

Recently we investigated the formation of liquid-crystalline mesophases in a fluid of hard spherocylinders, i.e., cylindrical segments of length $L$ and diameter $D$ capped at each end by a hemisphere of the same diameter.[1] More specifically, we analyzed the ordering of the homogeneous and isotropic fluid into a nematic, smectic, or solid phase within the framework provided by the one-phase entropy-based criterion originally proposed by Giaquinta and Giunta.[2] This criterion can be implemented through the well-known multiparticle correlation expansion of the configurational entropy:[3]

$$s_{ex} = \sum_{n=2}^{\infty} s_n \tag{1}$$

In the above formula $s_{ex}$ is the excess entropy per particle in units of the Boltzmann constant and $s_n$ is the $n$-body entropy that is obtained upon resumming spatial correlations between up to $n$ particles. In particular, the pair entropy per particle of a homogeneous and isotropic fluid of nonspherical molecules can be written as[4]

$$s_2(\rho) = -\frac{1}{2}\frac{\rho}{\Omega^2}\int \{g(\mathbf{r},\omega^2)\ln[g(\mathbf{r},\omega^2)] - g(\mathbf{r},\omega^2) + 1\}\, d\mathbf{r}\, d\omega^2 \tag{2}$$

where $g(\mathbf{r},\omega^2)$ is the pair distribution function (PDF) that depends on the relative separation $\mathbf{r}$ between two molecules and on the set of Euler angles $\omega^2 \equiv [\omega_1,\omega_2]$ that specifies their absolute orientations in the laboratory reference frame. The quantity $\Omega$ represents the integral over the Euler angles of one molecule, and $\rho$ is the particle number density.

To identify the ordering threshold of the fluid, we monitor the behavior (as a function of the number density) of the so-called residual multiparticle entropy (RMPE). This quantity is defined as the difference

$$\Delta s \equiv s_{ex} - s_2 \tag{3}$$

At variance with the pair entropy, the RMPE exhibits a nonmonotonic behavior as a function of $\rho$. In particular, it is negative at low densities and becomes positive as a more ordered phase is approached. The relevance of the condition $\Delta s = 0$ as a one-phase ordering criterion has been documented for a variety of phase transitions undergone by continuous fluids as well as by lattice gases.[5]

Even for systems composed of nonspherical molecules, such as hard spherocylinders, it turns out that the ordering thresholds detected by the zero-RMPE condition systematically correlate with the corresponding phase-transition points, whatever the nature of the higher density phase coexisting with the isotropic fluid.[1] Cuetos and co-workers have successfully applied the RMPE criterion to hard spherocylinders with an attractive square well and to spherocylinders with a soft repulsive core as well.[6]

In this paper we intend to analyze the predictions of the RMPE approach in the case of the nematic-smectic transition undergone by parallel hard spherocylinders with aspect ratio $L/D = 5$. The onset of smectic order out of a nematic phase represents the next step in the process that, upon compression of the isotropic fluid, eventually leads to the formation of the fully crystalline solid. The phase behavior of this model has been investigated with several numerical simulations[7−9] as well as theoretical studies (see, e.g., refs 10−14) over the whole $L/D$ range. Such studies have ascertained the existence of a second-order phase transition from a low-density nematic state to an intermediate smectic phase. On the other hand, the general features of the higher density region of the phase diagram has long been debated as far as the stability a columnar phase is concerned.[8]

* Corresponding author. E-mail: Paolo.Giaquinta@unime.it.
† INFM and Università degli Studi di Messina.
‡ CNR.

10.1021/jp0345001 CCC: $25.00 
Published on Web 07/29/2003

Since the seminal work of Onsager,[15] the model of either parallel or freely rotating hard spherocylinders has provided a suitable framework, notwithstanding its simplicity, for investigating entropy-driven mesophase formations in real colloidal fluids composed of rigid rodlike molecules.[16] More recently, theoretical studies[17] and computer simulation investigations[18] have also been carried out for a dispersion of parallel spherocylinders in a solvent of hard spheres. A renewed interest in these model mixtures came from the experimental observations of the variegated phase behavior exhibited by some complex fluids such as those composed of viruses and spherical polymeric particles.[19] The observed phenomenology has features that can be relevant for understanding the properties of low-molecular-mass liquid crystals[20] as well as of polymeric and biological systems.[21,22]

The paper is organized as follows: In sections 2 and 3 we describe the theoretical framework and the numerical simulation technique. The results are presented in section 4 and section 5 is devoted to concluding remarks.

## 2. Theory

The formalism developed in ref 1 for the isotropic fluid needs to be modified to describe the nematic and smectic mesophases. Even for uniaxial molecules, the numerical computation of the full pair distribution function $g(\mathbf{r},\omega^2)$ is a formidable task. Costa and co-workers have already shown that, to reproduce the phase boundaries of the isotropic fluid, it is enough to take into account the dependence of $g(\mathbf{r},\omega^2)$ on the centers-of-mass separation $r$ and on the angle $\theta$ formed by the molecular axes of two spherocylinders.[1] This angle shows up as the critical parameter, which accounts, by itself, for the reduction of orientational states that is ultimately offset by the gain of translational entropy at high densities.[15] On the other hand, it is rather obvious that the angle $\theta$ conveys no useful information on the structural process that may eventually lead to the formation of a smectic phase out of a nematic phase.

To resolve ordering effects associated with the orientational degrees of freedom on one side and with the modulation of the density along the nematic director on the other side, we shall restrict our analysis to a system composed of parallel spherocylinders. Assuming that the molecules are perfectly aligned does not significantly alter the main aspects of the phenomenology that we want to investigate. As emphasized above, different mechanisms drive the phase transformation of an isotropic or of a nematic fluid into a more ordered phase. Moreover, at the nematic−smectic transition threshold the nematic fluid is typically characterized by a very high degree of relative alignment of the molecules. For example, the nematic order parameter is about 0.85−0.89 for spherocylinders with aspect ratio $L/D = 5$.[23] The constraint on the relative orientation of the particles hugely simplifies the expression of the PDF. In fact, to specify the spatial configuration of a given spherocylinder relative to that fixed at the origin, one just needs two parameters: the distance $r$ and the angle $\vartheta$ formed by $\mathbf{r}$ and by the nematic director. The other polar angle $\phi$ is actually averaged out on account of the macroscopic cylindrical symmetry of the model. We emphasize that in this case, at variance with the freely rotating model already investigated in ref 1, no approximation is needed to compute the PDF of the system. Correspondingly, the pair entropy of the fluid can be written as

$$s_2(\rho) = -\pi\rho\int_0^\infty r^2\,\mathrm{d}r\int_0^\pi \sin\vartheta\,\mathrm{d}\vartheta\,\{g(r,\vartheta)\ln[g(r,\vartheta)] - g(r,\vartheta) + 1\} \quad (4)$$

Using a formalism analogous to that introduced in ref 1, we extract from eq 4 the excluded-volume contribution to the pair entropy of the fluid. This contribution arises from the space integration carried out over the regions where $g(r,\vartheta) = 0$:

$$s_2 = -B_2\rho + s'_2 \quad (5)$$

In eq 5 $B_2$ is the second virial coefficient of hard parallel spherocylinders that is just 4 times the volume, $V_{hsc}$, of a spherocylinder:

$$B_2 = 4[(\pi/4)D^2L + (\pi/6)D^3] \quad (6)$$

The residual contribution, $s'_2$, explicitly accounts for the decrease of the pair entropy associated with the onset of interparticle correlations at short and medium-range distances. For parallel spherocylinders, a further separation of this term into a translational and an orientational contribution (as done in ref 1) does not make much sense.

The total excess entropy of the nematic fluid can be evaluated upon integrating the equation of state (EoS):

$$s_{ex}(\rho) = s_{ex}(\bar\rho) - \int_{\bar\rho}^{\rho}\left[\frac{\beta P}{\rho'} - 1\right]\frac{\mathrm{d}\rho'}{\rho'} \quad (7)$$

In eq 7 $P$ is the pressure, $\beta$ is the inverse temperature in units of the Boltzmann constant, and $\bar\rho$ is the density of a suitably chosen reference state. The EoS of the fluid was obtained through a Monte Carlo sampling of the system at different pressures, whereas the quantity $s_{ex}(\bar\rho)$ was calculated using the Widom test-particle insertion method[24,25] to evaluate the excess chemical potential, $\mu_{ex}$, at low enough densities. The excess entropy can then be obtained through the thermodynamic equation:

$$s_{ex} = -\beta\mu_{ex} + \frac{\beta P}{\rho} - 1 \quad (8)$$

## 3. Simulation

We investigated the phase diagram of a system of parallel hard spherocylinders with elongation $L/D = 5$, spanning a density range from a rather dilute nematic state up to the smectic transition threshold. We carried out Monte Carlo (MC) simulations at constant pressure, as is usual for systems of nonspherical hard-core particles where it may be difficult to calculate the equation of state in a constant-volume simulation through the contact values of the distribution functions.[25]

The typical sample was composed of $N = 1500$ particles, aligned along the $z$ axis and enclosed in an orthorhombic box with edges $L_x = L_y = {}^1/_3L_z$. To quantify the influence of the size of the system as well as of the shape of the simulation box, we also investigated the behavior of a system composed of 500 particles aligned along the main diagonal of a cubic box and of a fluid of 768 particles enclosed in a orthorhombic cell with the same relative dimensions used for the main sample.

All thermodynamic isobaric states were sequentially generated from a translationally disordered low-density configuration upon gradually compressing the nematic fluid. The equilibration period was typically $10^5$ MC cycles, a cycle consisting of an attempt to change sequentially the center-of-mass coordinates of each molecule followed by an attempt to modify the volume of the sample. Simulation data were obtained by generating chains consisting of $5 \times 10^5$ to $20 \times 10^5$ MC cycles, depending on the pressure. Equilibrium averages and standard deviations were computed by dividing chains into independent blocks. During the production runs, we cumulated different histograms

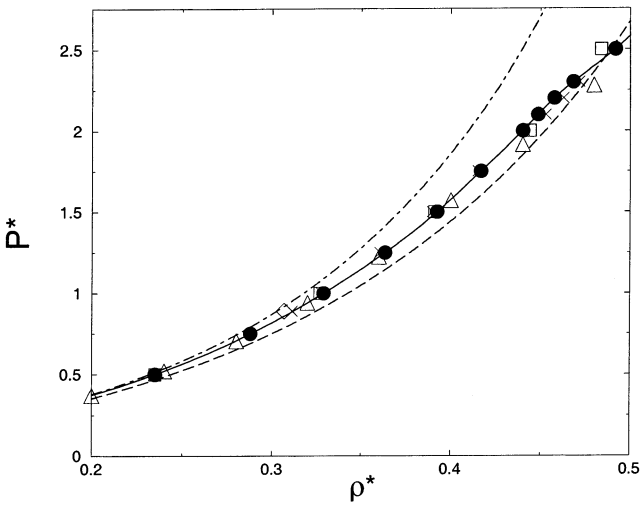


**Figure 1.** Equation of state of parallel hard spherocylinders with aspect ratio $L/D = 5$. Line with solid circles and crosses: this work for $N = 1500$ and $N = 500$ molecules, respectively. Triangles, squares, and diamond: simulations by Veerman and Frenkel,[8] Stroobants and co-workers,[7] and Koda and Ikeda,[9] respectively. The error bars are systematically smaller than the size of the markers. We also included, for comparison, the analytical equations of state proposed by Cotter and Martire[14] (dash−dotted line) and by Koda and Ikeda[9] (dashed line), respectively.

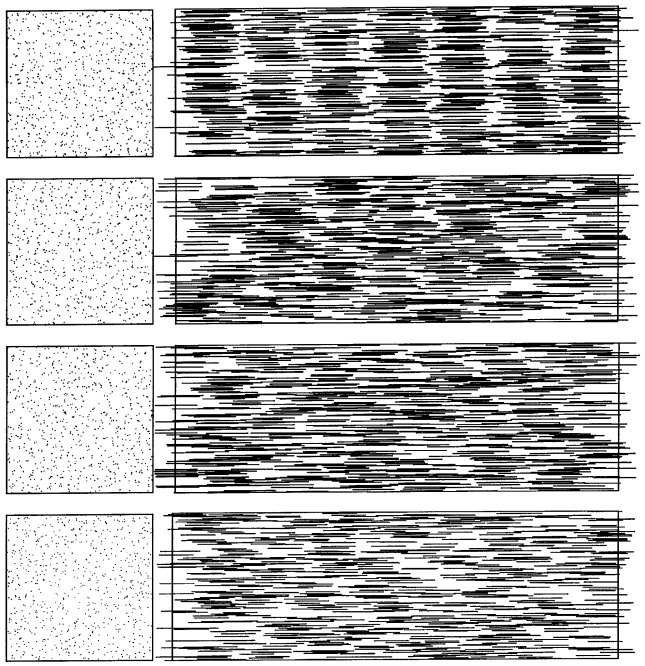

**Figure 2.** Snapshots of equilibrated configurations for (from top to bottom) $P^* = 2.50$ ($\langle\rho^* = 0.49\rangle$), $P^* = 2.30$ ($\rho^* = 0.47\rangle$), $P^* = 2.00$ ($\langle\rho^* = 0.44\rangle$), and $P^* = 0.50$ ($\langle\rho^* = 0.23\rangle$). Left panels: projections of the centers of mass of the spherocylinders onto the $x-y$ plane. Right panels: configurations along the $z$ axis.

of the PDF. In particular, $g(r,\vartheta)$ was sampled at intervals $\Delta r$ and $\Delta\vartheta$ of $0.05D$ and 1°, respectively. Different choices of $\Delta r$ and $\Delta\vartheta$ were also investigated for $P^* = 1.0$ and $P^* = 2.0$. As for the Widom insertion method, 100 trial insertions per MC cycle turned out to be sufficient to ensure a stable statistics for the excess chemical potential of the fluid.

In the presentation of the results, we shall refer to the reduced density $\rho^* = \rho/\rho_{cp}$, where $\rho_{cp} = 2/[\sqrt{2} + (L/D)\sqrt{3}]$ is the maximum density attained by parallel spherocylinders at close packing, and to the reduced pressure $P^* = \beta P V_{hsc}$.

## 4. Results

The current MC results for the EoS of the model are presented in Figure 1. The comparison between the data collected for 1500 particles (in an orthorombic box) and those for 500 particles (in a cubic box) shows that the EoS of the fluid is rather weakly affected by the size and the shape of the sample only at high densities. The results for 768 particles in an orthorombic box were not reported in the graph because they can be hardly resolved from those pertaining to the largest size investigated. The present EoS is in good agreement with that computed by other authors[7,9] over the whole density range explored, apart from a modest deviation, at high densities, from the molecular-dynamics results obtained by Veerman and Frenkel.[8] These authors as well as Stroobants and co-workers[7] noted a weak change of slope in the EoS at the transition that was estimated to occur for $\rho^* = 0.46$. Other structural properties of the system were evaluated in ref 7, such as the distribution functions associated with parallel and perpendicular correlations, below and above the observed cusp. Given the absence of either translational order within the layers or hysteresis effects associated with a compression/expansion cycle, Stroobants and co-workers concluded that the nematic phase actually transforms into a smectic phase through a continuous phase transition. Veerman and Frenkel later estimated the transition density by studying the critical slowing down of the intermediate scattering function evaluated along the nematic director.[8] Their result agrees with that reported by Stroobants and co-workers.[7] We also show in Figure 1 the analytical approximations for the EoS of the model that were suggested by Cotter and Martire[14,26] and, more recently, by Koda and Ikeda.[9] Both approximations were derived within the framework of scaled-particle theory for rodlike particles. The EoS proposed by Koda and Ikeda significantly improves over the approximation proposed by Cotter and Martire and provides a reliable representation of the compressibility factor of parallel spherocylinders over a wide range of densities and aspect ratios.

We verified that the system spontaneously transforms, during the simulation, into a smectic fluid, as can be also seen through the snapshots of equilibrated configurations that are shown in Figure 2. Such snapshots were taken for densities across the transition threshold. Traces of smectic order can be hardly detected for $P^* = 2.00$, a pressure corresponding to an average reduced density of 0.44. The ordering of the fluid is already apparent just beyond the transition threshold for $P^* = 2.30$ and $\rho^* \simeq 0.47$. Fully developed arrangements of several well-separated smectic layers distributed along the $z$ direction are clearly visible for $P^* = 2.50$ and $\rho^* \simeq 0.49$. Instead, the transversal arrangements of the spherocylinders along the $x-y$ plane look disordered in all states investigated (compare left and right panels in Figure 2).

We show in Figure 3 the excess entropy of the fluid plotted as a function of the reduced density. The data were obtained using both the thermodynamic integration of eq 7 and Widom's ghost-particle method implemented at moderately low densities. We also show the datum recently reported by Koda and Ikeda,[9] which was obtained using a multistage Widom test, based on the gradual insertion of a ghost particle with a variable shape. The modest discrepancy between this finding and the present results is likely due to the multistage method, which is known to work better at higher densities. On the other hand, our results for the excess entropy are closely interpolated by the expression

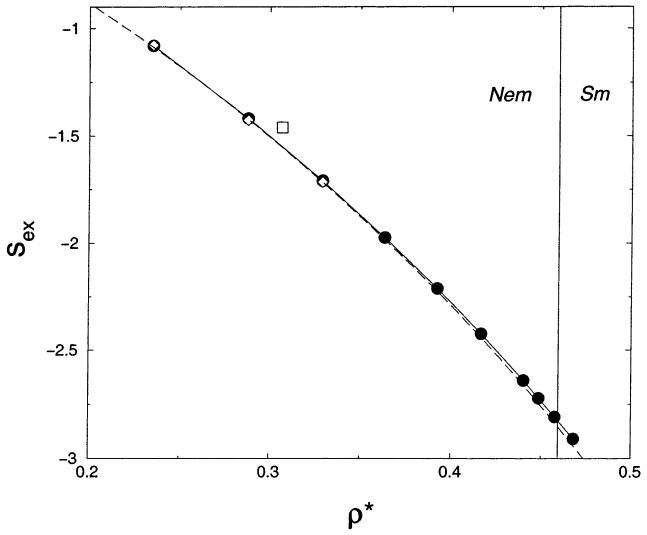


**Figure 3.** Excess entropy plotted as a function of the reduced density: line with solid circles, this work with $N = 1500$; diamonds, Widom insertion-method estimates; square, multistage Widom test;[9] dashed line, excess entropy evaluated by integration of the five-term virial fit of the simulation data of ref 7. The vertical line indicates the nematic−smectic transition threshold according to refs 7 and 8.

obtained upon integrating the five-term virial fit of the EoS reported in ref 7.

The PDF of the fluid, $g(r,\vartheta)$, was plotted in Figure 4 as a function of $\vartheta$ for a set of interparticle distances at increasing pressures across the transition point ($P^* \simeq 2.2$). We note, for separations $r < L + D$, the existence of a forbidden range around $\vartheta = 0$ and $\pi$ that is due to the overlap of two spherocylinders. This correlation gap decreases with increasing intermolecular separations. The maximum attained by $g(r,\vartheta)$ corresponds to the hard-core contact between spherocylinders, and its height consistently decreases with increasing interparticle distances. For $r \geq L + D$, the entire angular range between 0 and $\pi$ can be sampled by a second spherocylinder. Of course, the contact value of the PDF blows up for $\vartheta = 0$, $\pi$, and progressively decreases for increasing distances. An increase of the pressure enhances the overall structure of the PDF; however, no specific signature of the nematic−smectic transition can be detected in the resulting modification of the PDF.

Upon plugging the PDF into eq 4, we obtained the pair entropy that was plotted, together with the excess entropy, as a function of the density in Figure 5. The RMPE exhibits a change of sign from negative to positive values for $\rho^* \simeq 0.453$. This threshold practically coincides with the currently accepted nematic−smectic transition density ($\rho^* = 0.46$).[7,8] The simulations carried out for 500 particles enclosed in a cubic box show a similar behavior of the RMPE whose morphology is not substantially modified with respect to that of 1500 spherocylinders in an orthorombic box. This finding is noteworthy in that it demonstrates the high sensitivity of the RMPE to the structural changes occurring in the fluid, irrespective of the difficulty to accommodate a well-resolved smectic layering in a relatively small cubic box.

Figure 6 shows the quantity that, upon integration, yields the pair entropy in eq 4. For very short interparticle distances the $\vartheta$ range that can be sampled by two neighboring particles is rather limited. As a result, angular correlations are strong and give rise to the deep well in the integrand function. A steady modulated increase follows up to $r = L + D$, where a negative jump witnesses the onset of new strong correlations between spherocylinders lying on top or below the central reference

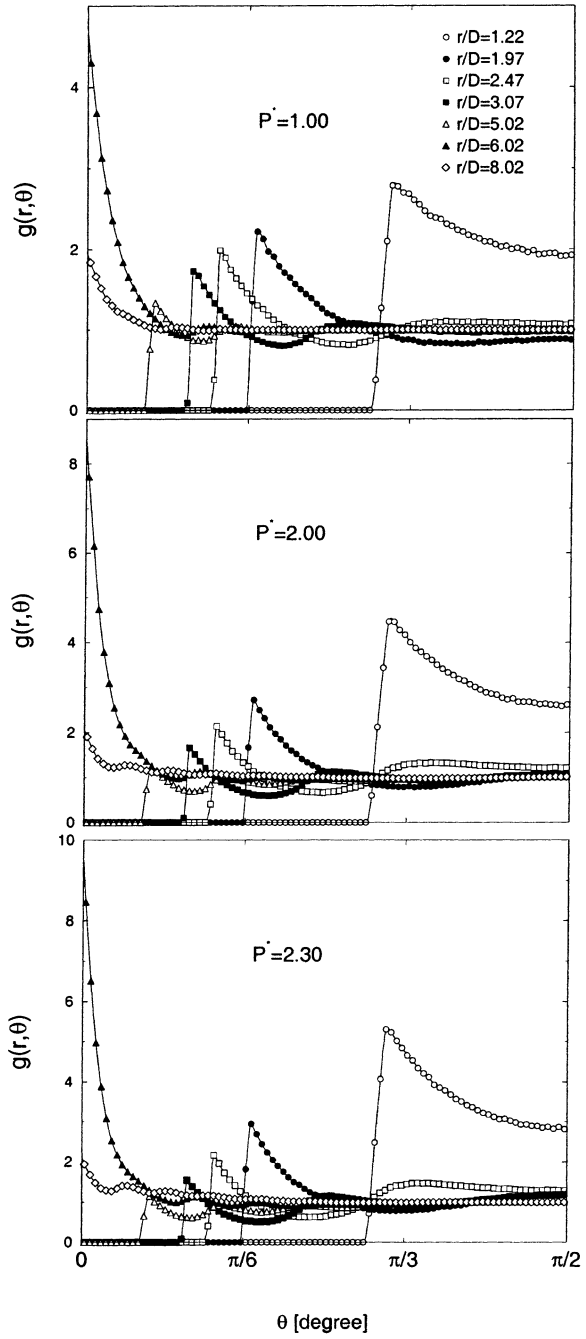


**Figure 4.** Pair distribution function $g(r,\vartheta)$ plotted as a function of $\vartheta$ for different distances $r/D$ and for increasing pressures.

particle. This effect is the integrated counterpart of the behavior that was already discussed for $g(r,\vartheta)$ in Figure 4.

The pair entropy was finally resolved into an excluded-volume and a correlation term in Figure 7 (see eq 5). It is clear that the second-order virial term cannot account by itself for the crossover between $s_{ex}$ and $s_2$ that is indicative of the smectic ordering of the nematic fluid.

As for the numerical reliability of the current results, we note that the statistics cumulated on $g(r,\vartheta)$ was such that a smooth integration over the sampled points yielded rather stable values for $s_2$, the dispersion being always lower than 1% of the average value. However, we observed a moderate sensitivity of the angle-dependent quantities in eq 4 on the resolution of the angular width $\Delta\vartheta$. To gain a better insight into the numerical accuracy of the calculations, we performed a series of test runs

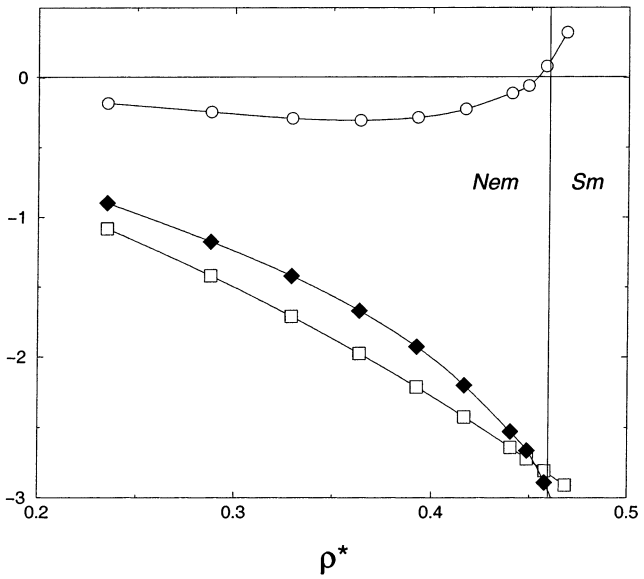


**Figure 5.** Residual multiparticle entropy (circles) resolved into the excess (squares) and pair (solid diamonds) contributions. Lines are smooth interpolations of the simulation data.

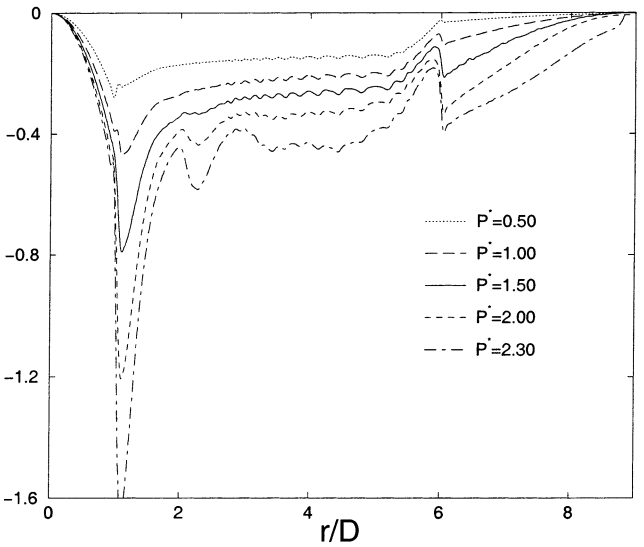


**Figure 6.** Integrand function appearing in eq 4, after integration over $\vartheta$, plotted for several pressures.

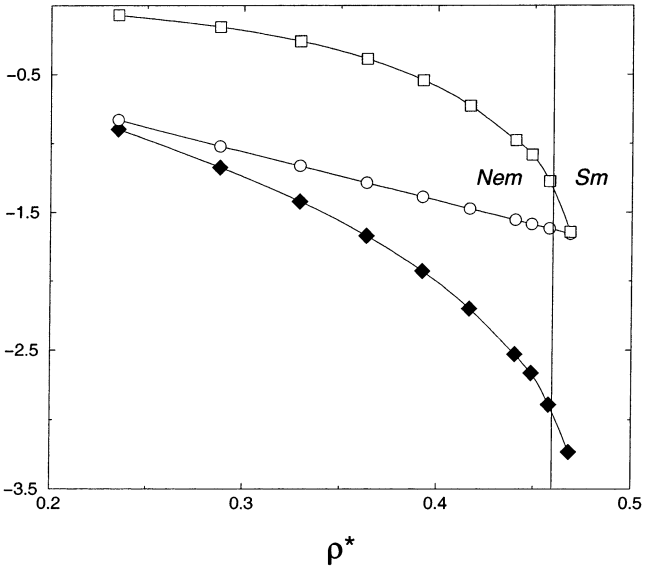


**Figure 7.** Pair entropy (diamonds) resolved into the excluded-volume (circles) and correlation (squares) contributions (see eq 5). Lines are smooth interpolations of the simulation data.

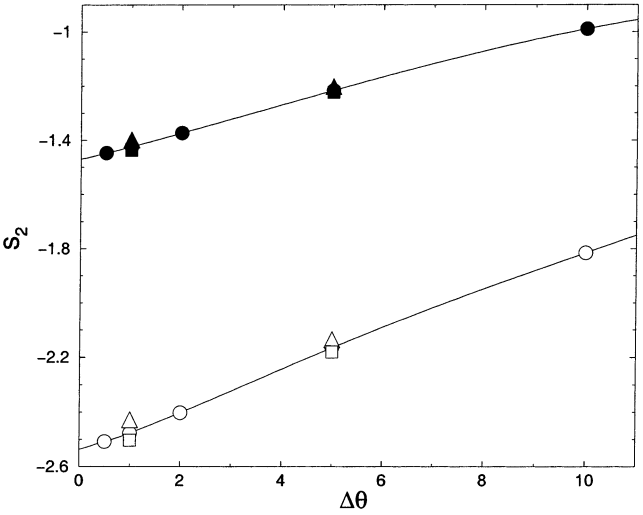


**Figure 8.** Pair entropy $s_2$ plotted as a function of the grid mesh parameter $\Delta\vartheta$ and for several choices of $\Delta r$, for $P^* = 1.00$ (solid symbols) and $P^* = 2.00$ (open symbols). Key: triangles, $\Delta r = 0.10D$; circles, $\Delta r = 0.05D$; squares, $\Delta r = 0.02D$.

for two different pressures ($P^* = 1.0$ and 2.0) with several $r$ and $\vartheta$ grid meshes. The tests were reported in Figure 8, where the higher sensitivity of $s_2$ on the angular grid size, as compared with the radial one, is manifest. We estimated, in the 2-fold limit of $\Delta r$ and $\Delta\vartheta \rightarrow 0$, an asymptotic shift of $s_2$ toward lower values not larger than 2%. As a result, we expect a comparable shift of the transition threshold signaled by the RMPE to lower densities.

## 5. Concluding Remarks

In this paper we have analyzed the residual multiparticle entropy (RMPE) of parallel hard spherocylinders with aspect ratio $L/D = 5$ across the nematic−smectic transition. The correspondence between the intrinsic ordering threshold detected through the vanishing of the RMPE ($\rho^* \simeq 0.453$) and the independently ascertained phase-transition density ($\rho^* = 0.46$) is quantitative. It also turned out that the indication of the zero-RMPE criterion is not significantly affected by the size and shape of the simulation box, even when the smectic layering of the fluid cannot be easily accommodated in the sample, as is the case of a small cubic box. This finding further corroborates the sensitivity of the RMPE to the ordering of the fluid on a local scale.

We intend to merge the formalism developed in ref 1 for the phase transitions undergone by the isotropic fluid with the present approach for the nematic−smectic transition, so as to achieve a flexible and unified tool to investigate the formation of liquid-crystalline mesophases in systems of elongated particles. We further plan to apply the RMPE criterion to mixtures of hard rods and spherical particles, a model of current interest for the chemical physics of real colloidal systems,[19] for which some preliminary simulation results are already available.[18]

## References and Notes

(1) Costa, D.; Micali, F.; Saija, F.; Giaquinta, P. V. *J. Phys. Chem. B* **2002**, *106*, 12297. Costa, D.; Saija, F.; Giaquinta, P. V. *Chem. Phys. Lett.* **1998**, *283*, 86; **1999**, *299*, 252 (erratum).

(2) Giaquinta, P. V.; Giunta, G. *Physica A* **1992**, *187*, 145.
(3) Nettleton, R. E.; Green, M. S. *J. Chem. Phys.* **1958**, *29*, 1365.
(4) Lazaridis, T.; Paulaitis, M. E. *J. Phys. Chem.* **1992**, *96*, 3847; **1994**, *98*, 635.
(5) Saija, F.; Prestipino, S.; Giaquinta, P. V. *J. Chem. Phys.* **2001**, *115*, 7586 and references contained therein.
(6) Cuetos, A.; Martinez-Haya, B.; Rull, L. F.; Lago, S. *J. Chem. Phys.* **2002**, *117*, 2934; **2002**, *117*, 11405 (erratum).
(7) Stroobants, A.; Lekkerkeker, H. N. W.; Frenkel, D. *Phys. Rev. A* **1987**, *36*, 2929.
(8) Veerman, J. A. C.; Frenkel, D. *Phys. Rev. A* **1991**, *43*, 4334.
(9) Koda, T.; Ikeda, S. *J. Chem. Phys.* **2002**, *116*, 5825.
(10) Xu, H.; Lekkerkerker, H. N. W.; Baus, M. *Europhys. Lett.* **1992**, *17*, 163.
(11) Holyst, R.; Poniewierski, A. *Phys. Rev. A* **1991**, *39*, 2742.
(12) Taylor, M. P.; Hentsche, R.; Herzfeld, J. *Phys. Rev. Lett.* **1989**, *62*, 800.
(13) Hosino, M.; Nakano, H.; Kimura, H. *J. Phys. Soc. Jpn*. **1979**, *46*, 1709.
(14) Cotter, M. A.; Martire, D. E. *J. Chem. Phys.* **1970**, *52*, 1909.
(15) Onsager, L. *Ann. N. Y. Acad. Sci.* **1949**, *51*, 627.
(16) For a review see, e.g.: Lekkerkerker, H. N. W.; Buining, P.; Buitenhuis, J.; Vroege, G. J.; Stroobants, A. In Proceedings of the NATO-ASI *Observation, Prediction and Simulation of Phase Transitions in Complex Fluids*; Baus, M., Rull, L. F., Ryckaert, J. P., Eds.; Kluwer: Dordrecht, 1994; pp 53−112. Fraden, S. In Proceedings of the NATO-ASI *Observation, Prediction and Simulation of Phase Transitions in Complex Fluids*; Baus, M., Rull, L. F., Ryckaert, J. P., Eds.; Kluwer: Dordrecht, 1994; pp 113−164.
(17) Koda, T.; Numajiri, M.; Ikeda, S. *J. Phys. Soc. Jpn*. **1996**, *65*, 3551.
(18) Dogic, Z.; Frenkel, D.; Fraden, S. *Phys. Rev. E* **2000**, *62*, 3925.
(19) Adams, M.; Dogic, Z.; Keller, S. L.; Fraden, S. *Nature* **1998**, *393*, 349.
(20) Rieker, T. P. *Liq. Cryst.* **1995**, *19*, 497.
(21) Gelbart, W. M., Ben-Shaul, A., Roux, D., Eds. *Mycelles, Membranes, Microemulsions, and Monolayers*; Springer: New York, 1994.
(22) Adams, M.; Fraden, S. *Biophys. J.* **1998**, *74*, 669.
(23) McGrother, S. C.; Williamson, D. C.; Jackson, G. *J. Chem. Phys.* **1996**, *104*, 6755.
(24) Widom, B. *J. Chem. Phys.* **1963**, *39*, 2808.
(25) Frenkel, D.; Smit, B. *Understanding Molecular Simulation*; Academic Press: London, 1996.
(26) Cotter, M. A.; Martire, D. E. *J. Chem. Phys.* **1970**, *53*, 4500. Cotter, M. A. *Phys. Rev. A* **1974**, *10*, 625.